ISSN 1070-3284, Russian Journal of Coordination Chemistry, 2021, Vol. 47, No. 12, pp. 922–931. © Pleiades Publishing, Ltd., 2021.

The Length of Substituents on Ligands Regulates the Structural Diversity of Coordination Polymers

C. L. Zhang[a], *, J. L. Qian[a], T. Zhou[a], and Y. Q. Li[b], **

[a] *AnHui Province Key Laboratory of Optoelectronic and Magnetism Functional Materials, Key Laboratory of Functional Coordination Compounds of Anhui Higher Education Institutes, Anqing Normal University, Anqing, 261433 P.R. China*

[b] *State Key Laboratory of Polyolefins and Catalysis, Shanghai Key Laboratory of Catalysis Technology for Polyolefins, Shanghai Research Institute of Chemical Industry Co., Ltd., Shanghai, 200062 P.R. China*

**e-mail: clzhang@nju.edu.cn*

***e-mail: liyongqing@srici.cn*

Received October 13, 2020; revised March 26, 2021; accepted March 29, 2021

Abstract—Three coordination polymers, namely, $\{[Co(L^1)(HBTC)]\cdot 0.5L^1\}_n$ (**I**), $\{[Co(L^2)(HBTC)]\cdot H_2O\}_n$ (**II**), $\{[Co(L^3)(HBTC)]\cdot H_2O\}_n$ (**III**), have been synthesized based on three semi-rigid nitrogen-containing ligands (L^1 = 4,4'-(2,5-dimethoxy-1,4-phenylene)dipyridine; L^2 = 4,4'-(2,5-diethoxy-1,4-phenylene)dipyridine; L^3 = 4,4'-(2,5-dibutoxy-1,4-phenylene)dipyridine) and 1,3,5-benzenetricarboxylic acid (H_3BTC). Both **I** and **II** are a 4-connected uninodal sql net with point symbol $\{4^4\cdot 6^2\}$, **III** is a 6-connected uninodal rob net with point symbol $\{4^8\cdot 6^6\cdot 8\}$. The complexes were characterized by X-ray single-crystal diffraction (CIF files CCDC nos. 2034103 (**II**), 2034104 (**III**)), PXRD, IR spectra and TGA. Interestingly, the structural diversity of these complexes derived from the length of substituents on L^n (n = 1, 2, 3) ligands.

Keywords: coordination polymers, point symbol, semi-rigid ligand, substituent, structural diversity

DOI: 10.1134/S1070328421120058

INTRODUCTION

The development of coordination polymers (CPs) has attracted more and more attention for its application in gas adsorption and separation, photo- or electro-catalysis, fluorescent probes, proton conduction, drug delivery, etc. [1–7]. However, the first problem to be solved in this field is the rational design structures, which is influenced by many factors (organic ligands, metal ions, solvent system, pH value and reaction temperature, etc.) [8–13]. It is worth noting that the rational selection of organic ligands or coligands according to their lengths, rigidities, coordination modes and functional groups may provide the controllable CPs [14–17]. In various types of organic ligands, rigid ligands generally have conjugated systems and its structure is fixed; flexible ligands have complex structures and can rotate; semi-rigid ligands have the advantages of both rigid and flexible ligands, so they are favored by researchers in the synthesis of CPs [18, 19]. Nitrogen-containing ligands are a great variety and can be as an excellent hydrogen bond receptor [20, 21]. Different substituents on organic ligands also have great influence on the structure of CPs.

It is well known that organic carboxylic acids have rich network topology and broad application prospects, so the construction of coordination polymers using metal ion and anion O-donor ligands is one of the research hotspots in the field of crystal engineering [22]. In addition, carboxylic groups form highly unstable bonds with a series of metal cations, which is conducive to the formation of highly ordered, thermodynamic driven MOF structure rather than kinetically-favoured amorphous by-product [23]. In this regard, 1,3,5-benzenetricarboxylic acid (H_3BTC) as a well-known rigid ligand has yielded a large number of coordination polymers with fascinating structural features [24–27]. The three carboxyl groups of H_3BTC were evenly distributed around the benzene ring. Therefore, it can connect metal ions through a variety of coordination ways to form different skeletons. Additionally, H_3BTC can also form non covalent interaction, such as hydrogen bonds, π···π interactions and X–H···π (X = C, N, O) interactions due to the co-existence of carboxylate groups and the benzene ring. These weak interactions contribute to the formation of high dimensional supramolecular structures.

Three semirigid ligands with flexible functional groups, 4,4'-(2,5-dimethoxy-1,4-phenylene)dipyridine (L^1), 4,4'-(2,5-diethoxy-1,4-phenylene)dipyridine (L^2) and 4,4'-(2,5-dibutoxy-1,4-phenylene)-dipyridine (L^3), have been used to construct novel CPs in this work, namely, $\{[Co(L^1)(HBTC)]\cdot 0.5L^1\}_n$ (**I**)

(has been reported by ourselves) [28], $\{[Co(L^2)(HBTC)]\cdot H_2O\}_n$ (**II**), $\{[Co(L^3)(HBTC)]\cdot H_2O\}_n$ (**III**). The crystal structures and topological analyses are discussed. Furthermore, the structural diversity of three CPs derived from the length of substituents on L^n (n = 1, 2, 3) ligands is investigated in detail.

EXPERIMENTAL

Materials and methods. All reagents and solvents were purchased from commercial sources and used without further purification. The synthesis method of L^n (n = 1, 2, 3) ligands were synthesized based on previous reports with proper modifications [29]. The IR absorption spectra of these complexes and H_2L ligand were recorded in the range of 400–4000 cm^{-1} by means of a Nicolet (Impact 410) spectrometer with KBr pellets. Element analyses (C, H, N) were carried out on a Perkin-Elmer model 240C analyzer. Powder X-ray diffraction (PXRD) measurements were performed on a Bruker D8 Advance X-ray diffractometer using MoK_α radiation (λ = 0.71073 Å), in which the X-ray tube was operated at 40 kV and 30 mA. Thermogravimetric analysis (TGA) was performed under a N_2 atmosphere with a heating rate of 10 K min^{-1} by using a SDTQ600 thermogravimetric analyzer, and the crucible material is Al_2O_3.

Determination of crystal structures. X-ray crystallographic data were collected on a Bruker Apex Smart CCD diffractometer with graphite-monochromated MoK_α radiation (λ = 0.71073 Å). Structure was solved by direct method and the non-hydrogen atoms were located from the trial structure and then refined anisotropically with SHELXTL using full-matrix least-squares procedures based on F^2 values. A semiempirical absorption correction was applied using SADABS [30]. The hydrogen atom positions were fixed geometrically at the calculated distances and allowed to ride on the parent atoms. Crystal data, data collection and structure refinement details are summarized in Table 1 and the key bond lengths and bond angles are given in Tables 2 and 3. All H atoms were positioned geometrically and refined using a riding model with C–H = 0.97 (CH_2) or 0.93 Å (aromatic ring) and U_{iso} (H) = 1.2U_{eq} (C), and O–H = 0.82 Å and U_{iso} (H) = 1.5 U_{eq} (O). The topological analysis was performed using the TOPOS program [31]. Computer programs: APEX2 [32], CrysAlis PRO [33], SAINT [31], SHELXT2016 [34], SHELXS97 [35], SHELXL2016 [36].

The full tables of atom coordinates, bond lengths, and bond angles are deposited with the Cambrideg Crystallographic Data Center (CIF files CCDC nos. 2034103 (**II**), 2034104 (**III**); deposit@ccdc.cam.ac.uk; http://www.ccdc.cam.ac.uk/structures).

Synthesis of complex I. A mixture of $Co(NO_3)_2\cdot 6H_2O$ (29.10 mg, 0.10 mmol), L^1 (16.0 mg, 0.05 mmol) and H_3BTC (10.50 mg, 0.05 mmol) were dissolved in 8.0 mL of DMF : H_2O (4 : 4). The final mixture was placed in a Teflon vessel (15 mL) under autogenous pressure and heated at 85°C for 3 days and then cooled to room temperature. The red block crystals were obtained. The yield of the reaction was calcd. 61% based on L^1 ligand.

For $C_{36}H_{28}N_3O_9Co$ (**I**)

Anal. calcd., %	C, 61.23	H, 3.97	N, 5.95
Found, %	C, 60.86	H, 4.07	N, 5.75

This method is different from that in reference [28], but the yield is higher than it.

Synthesis of complex II. The synthetic method of **II** is similar to **I**, only the L^2 ligand replaced by L^3. The red block crystals were obtained. The yield of the reaction was calcd. 58% based on L^2 ligand.

For $C_{29}H_{26}N_2O_9Co$ (**II**)

Anal. calcd., %	C, 57.57	H, 4.30	N, 4.63
Found, %	C, 57.65	H, 4.24	N, 4.66

IR (ν, cm^{-1}): 3610.02, 3342.73, 3134.16, 2975.47, 2930.09, 1721.60, 1609.80, 1586.77, 1552.81, 1522.46, 1489.21, 1475.45, 1438.73, 1390.73, 1334.57, 1273.61, 1225.37, 1214.01, 1190.15, 1109.46, 1062.63, 1041.77, 1018.67, 931.44, 866.61, 837.31, 807.63, 794.98, 756.48, 723.55, 703.39, 682.16, 538.36, 432.33.

Synthesis of complex III. The synthetic method of **III** is similar to **I**, only the L^1 ligand replaced by L^3. Finally, the red block crystals **III** was obtained. The yield of **III** was about 56% (based on L^3 ligand).

For $C_{33}H_{34}N_2O_9Co$ (**III**)

Anal. calcd., %	C, 59.86	H, 5.14	N, 4.23
Found, %	C, 59.64	H, 5.24	N, 4.18

IR (ν, cm^{-1}): 3423.21, 3338.56, 3090.92, 2959.07, 2873.94, 1722.34, 1636.88, 1608.95, 1551.83, 1522.87, 1488.30, 1473.76, 1431.47, 1389.22, 1308.72, 1279.62, 1220.16, 1104.12, 1060.79, 1035.84, 1016.75, 929.14, 909.52, 888.32, 840.83, 819.05, 799.30, 746.82, 720.75, 706.82, 691.60, 544.54, 474.89, 451.61, 418.35.

RESULTS AND DISCUSSION

For the structural description of **I**, please refer to reference [28]. Complex **II** crystallizes in the triclinic space group $P\bar{1}$. Its asymmetric unit contains one Co^{2+} ion, one L^2 ligand, one dianions of 1,3,5-benzenetricarboxylic acid and one free water molecule. Each Co(II) center is coordinated by two nitrogen atoms from two L^2 ligands and four carboxylate oxygen atoms from three BTC ligands in a irregular quadrangular bipyramid geometry (Fig. 1). The Co–O bond

Table 1. Crystallographic date and structure refinements of complexes **II** and **III**

Parameter	Value	
	II	**III**
Empirical formula	$C_{29}H_{26}N_2O_9Co$	$C_{33}H_{34}N_2O_9Co$
Formula weight	605.45	661.55
Crystal system	Triclinic	Monoclinic
Space group	$P\bar{1}$	$C2/c$
Temperature, K	293(2)	293(2)
a, Å	10.1177(6)	28.6049(10)
b, Å	10.8086(7)	13.0746(4)
c, Å	13.6407(8)	17.2426(6)
α, deg	78.7250(10)	
β, deg	74.6420(10)	105.6500(10)
γ, deg	76.4420(10)	
V, Å^3	1384.13(15)	6209.6(4)
Z	2	8
μ, mm^{-1}	0.678	0.611
Crystal size, mm	0.320 × 0.300 × 0.280	0.220 × 0.200 × 0.180
F(000)	626	2760
θ_{min}–θ_{max}, deg	1.564–27.661	1.479–27.509
T_{min}, T_{max}	0.805, 0.827	0.874, 0.896
Reflections collected/unique	12720, 6339	20714, 7141
R_{int}	0.0273	0.0211
N_{res}, N_{par}	0, 373	186, 417
R_1, wR_2 ($I > 2\sigma(I)$)	0.0354, 0.0881	0.0420, 0.1173
GOOF on F^2	1.031	1.090
Largest diff. peak and hole, e Å^{-3}	0.471 and –0.406	1.008 and –0.548

distances are 2.019(15)–2.254(16) Å, and the Co–N bond distances are 2.138(17) and 2.149(17) Å; the OCoO angles are in the range of 59.15(6)°–152.75(7)°, the NCoO angles are in the range of 86.35(7)°–94.58(7)°, and the NCoN angle is 173.83(7)°. The dianions of 1,3,5-benzenetricarboxylic acid acts as a μ_3-bridge linking three Co(II) atoms, in which one carboxylate group adopts the bidentate chelate mode and the other adopts a μ_2-η^1:η^1 fashion. The Co^{2+} ion is six-coordinated, the SBU is obtained through two –OCO-groups, and generate a dinuclear $Co_2(CO_2)_2$ SBU with a Co···Co separation of 4.1536(5) Å. These $Co_2(CO_2)_2$ SBUs are further bridged by $HBTC^{2-}$ ligands through the horizontal direction and L^2 ligands from the vertical direction to furnish a 2D network (Fig. 1b). By omitting the free water molecules, the structure can be simplified to a 4-connecting uninodal sql net (point symbol $4^4{\cdot}6^2$).

Complex **III** crystallizes in the monoclinic space group $C2/c$. Its asymmetric unit contains one Co^{2+} ion, one L^3 ligand, one dianions of 1,3,5-benzenetricarboxylic acid and one free water molecule. Each Co(II) center is coordinated by two nitrogen atoms from two L^3 ligands and four carboxylate oxygen atoms from three H_3BTC ligands in a irregular octahedral geometry [CoO_4N_2] (Fig. 2). The Co–O bond distances are 2.013(15)–2.250(16) Å, and the Co–N bond distances are 2.160(17) and 2.163(17) Å; the OCoO angles are in the range of 58.92(6)°–146.90(6)°, the NCoO angles are in the range of 84.43(7)°–98.84(7)°, and the NCoN angle is 176.52(7)°. The dianions of 1,3,5-benzenetricarboxylic acid was connected with three Co^{2+} ions to obtain

Table 2. Selected bond lengths (Å) for complexes **II** and **III***

Bond lengths (**II**)	Å	Bond lengths (**III**)	Å
Co(1)–O(3)$^{\#1}$	2.0224(12)	N(2)–Co(1)$^{\#1}$	2.1629(17)
Co(1)–O(4)$^{\#2}$	2.0377(12)	Co(1)–O(3)$^{\#2}$	2.0132(15)
Co(1)–N(2)	2.1376(14)	Co(1)–O(4)$^{\#3}$	2.0188(14)
Co(1)–N(1)	2.1492(14)	Co(1)–N(1)	2.1601(17)
Co(1)–O(2)	2.1683(13)	Co(1)–N(2)$^{\#4}$	2.1629(17)
Co(1)–O(1)	2.2551(13)	Co(1)–O(1)	2.1770(15)
O(3)–Co(1)$^{\#3}$	2.0223(12)	Co(1)–O(2)	2.2499(16)
O(4)–Co(1)$^{\#2}$	2.0376(12)	O(4)–Co(1)$^{\#5}$	2.0188(14)
		O(3)–Co(1)$^{\#6}$	2.0133(15)

* Symmetry transformations used to generate equivalent atoms: $^{\#1}$ $x-1, y, z$, $^{\#2}$ $-x+1, -y+1, -z$, $^{\#3}$ $x+1, y, z$ (**II**); $^{\#1}$ $x-1/2, y-1/2, z$, $^{\#2}$ $-x+1/2, y-1/2, -z+1/2$, $^{\#3}$ $x, -y+2, z+1/2$, $^{\#4}$ $x+1/2, y+1/2, z$, $^{\#5}$ $x, -y+2, z-1/2$, $^{\#6}$ $-x+1/2, y+1/2, -z+1/2$ (**III**).

Table 3. Selected bond angles (deg) for complexes **II** and **III***

Angle (**II**)	ω	Angle (**III**)	ω
O(3)$^{\#1}$Co(1)O(4)$^{\#2}$	117.51(5)	O(3)$^{\#2}$Co(1)O(4)$^{\#3}$	124.97(6)
O(3)$^{\#1}$Co(1)N(2)	87.65(5)	O(3)$^{\#2}$Co(1)N(1)	88.95(7)
O(4)$^{\#2}$Co(1)N(2)	94.49(6)	O(4)$^{\#3}$Co(1)N(1)	91.60(7)
O(3)$^{\#1}$Co(1)N(1)	86.49(6)	O(3)$^{\#2}$Co(1)N(2)$^{\#4}$	87.66(7)
O(4)$^{\#2}$Co(1)N(1)	89.35(6)	O(4)$^{\#3}$Co(1)N(2)$^{\#4}$	89.65(7)
N(2)Co(1)N(1)	174.01(6)	N(1)Co(1)N(2)$^{\#4}$	176.52(7)
O(3)$^{\#1}$Co(1)O(2)	152.63(5)	O(3)$^{\#2}$Co(1)O(1)	145.35(6)
O(4)$^{\#2}$Co(1)O(2)	89.85(5)	O(4)$^{\#3}$Co(1)O(1)	88.72(6)
N(2)Co(1)O(2)	91.03(6)	N(1)Co(1)O(1)	98.84(7)
N(1)Co(1)O(2)	93.58(6)	N(2)$^{\#4}$Co(1)O(1)	84.43(7)
O(3)$^{\#1}$Co(1)O(1)	93.51(5)	O(3)$^{\#2}$Co(1)O(2)	88.09(6)
O(4)$^{\#2}$Co(1)O(1)	148.75(5)	O(4)$^{\#3}$Co(1)O(2)	146.90(6)
N(2)Co(1)O(1)	90.27(5)	N(1)Co(1)O(2)	87.18(7)
N(1)Co(1)O(1)	88.82(5)	N(2)$^{\#4}$Co(1)O(2)	93.54(7)
O(2)Co(1)O(1)	59.15(5)	O(1)Co(1)O(2)	58.92(6)

* Symmetry transformations used to generate equivalent atoms: $^{\#1}$ $x-1, y, z$, $^{\#2}$ $-x+1, -y+1, -z$ (**II**); $^{\#2}$ $-x+1/2, y-1/2, -z+1/2$, $^{\#3}$ $x, -y+2, z+1/2$, $^{\#4}$ $x+1/2, y+1/2, z$ (**III**).

a 1D structure through bidentate chelation and bidentate bridging node, then the L^3 ligand was connected with the 1D structure in two different directions to form a 3D structure (Fig. 2). Two CoO_4N_2 polyhedrons are connected by two –OCO-groups to generate a dinuclear $Co_2(CO_2)_2$ SBU with a Co···Co separation of 4.0417(4) Å. From a topological perspective, the structure can be simplified to a 6-connecting uninodal rob net (point symbol $\{4^8{\cdot}6^6{\cdot}8\}$).

The PXRD pattern of complexes **II** and **III** are presented in Fig. 3. It can be seen that the diffraction peaks of the experimental patterns match well with the simulated ones. The result shows that the prepared samples have a high phase purity.

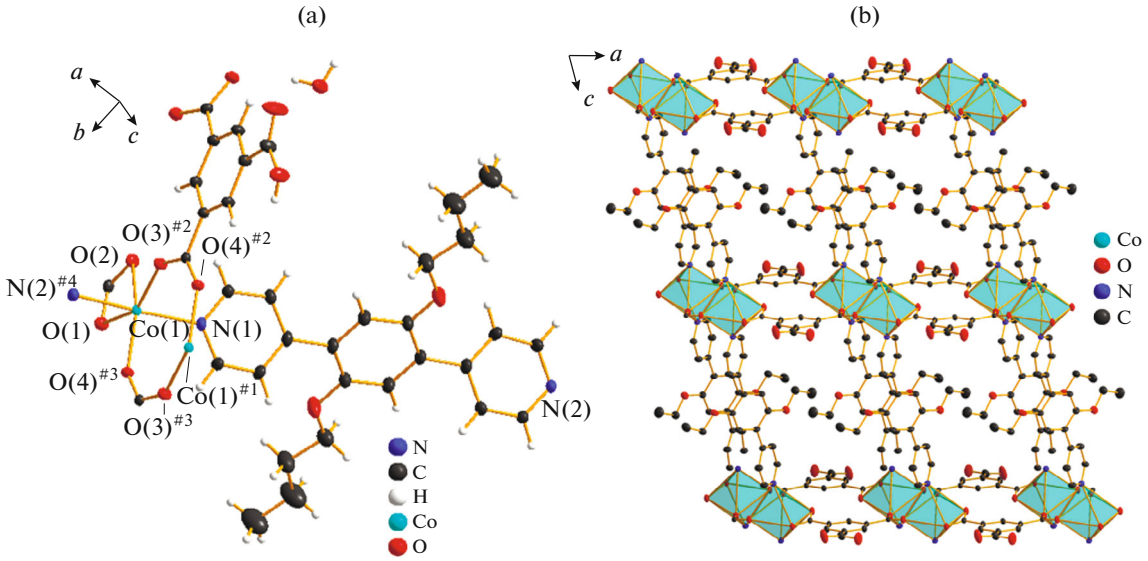

Fig. 1. Coordination environment of **II** with 30% ellipsoid probability (a); polyhedral representation of 2D network (b) (symmetry codes: $^{\#1}$ $-x, -y+1, -z$, $^{\#2}$ $x, y-1, z+1$, $^{\#3}$ $-x+1, -y+1, -z$, $^{\#4}$ $x-1, y, z$).

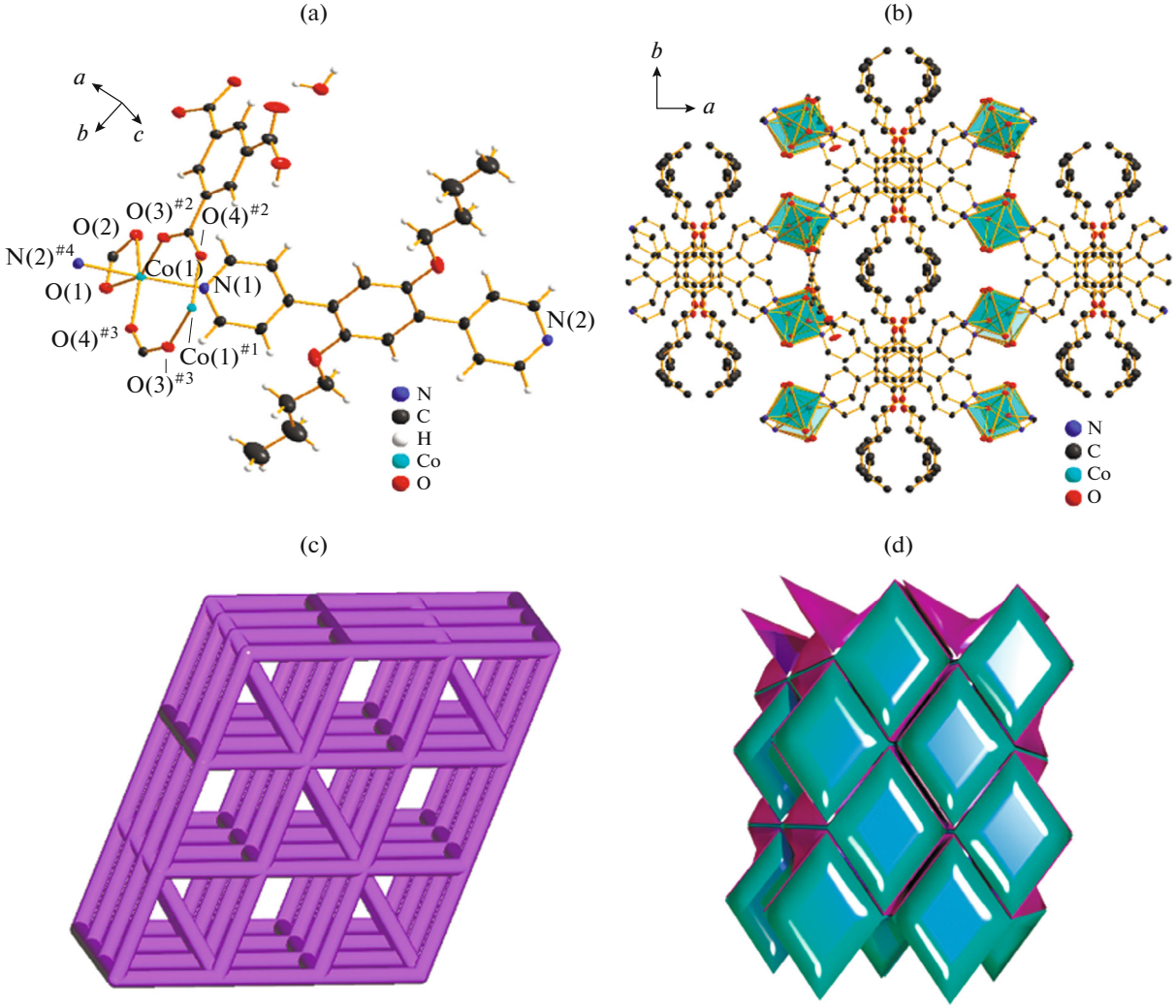

Fig. 2. Coordination environment of **III** with 30% ellipsoid probability (a); polyhedral representation of 3D network (b); 3D topology diagram (c); topological features of **III** displayed by tiling (d) (symmetry codes: $^{\#1}$ $-x+1/2, -y+3/2, -z+1$, $^{\#2}$ $-x+1/2, y-1/2, -z+1/2$, $^{\#3}$ $x, -y+2, z+1/2$, $^{\#4}$ $x+1/2, y+1/2, z$).

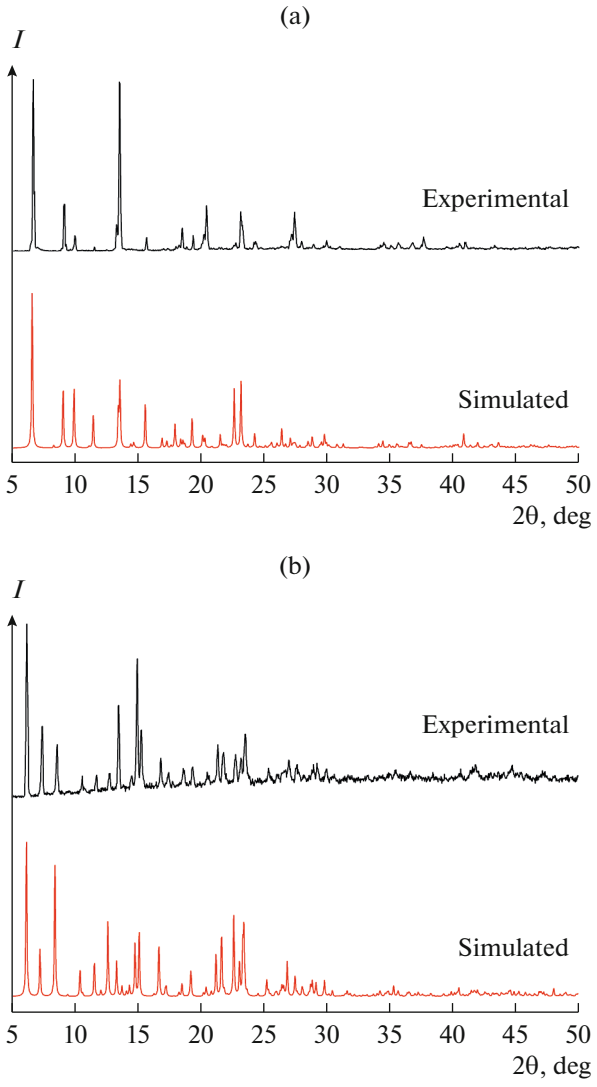

Fig. 3. The powder X-ray diffraction patterns of complexes **II** (a) and **III** (b).

The IR spectra of complexes **II**, **III**, ligand BTC, ligand L^2 and ligand L^3 were measured in the range 4000–400 cm^{-1} (Fig. 4).

TGA showed that the weight loss of 2.78% for complex **II** before 140°C corresponds to the loss of uncoordinated H_2O molecule (calcd. 2.97%). Until 420°C, a smooth curve appears, the sharply weight loss represents that the framework starts to decompose. Followed by the structure gradually collapse. The TG curve of complex **III** indicates that there is a weight loss of 2.83% before 150°C, which can be attributed to the loss of uncoordinated H_2O molecules (calcd. 2.72%), then a smooth curve appears. After 370°C, the rapid drop of weight indicates that the skeleton starts to destroy until it collapses (Fig. 5).

CPs **I**–**III** are constructed from semi-rigid nitrogen-containing ligands with different substituent length (methoxy for **I**, ethoxy for **II** and butyloxy for **III**), BTC ligands and the cobalt ions. One of the common characteristics of the three structures is that the dianions of 1,3,5-benzenetricarboxylic acid were coordinated with the three cobalt ions through bidentate chelation and bidentate bridging fashion, BTC lignads play an important role in the structure of complexes **I**–**III**. Nevertheless, there are different rings formed by BTC ligands and cobalt ions: ring A and ring B in structures **I** and **II**, only ring B in **III** (Figs. 6a, 6c, 6f). Compared with BTC, L^n ($n = 1, 2, 3$) ligands have a qualitative effect on the structure: (i) L^n ligands have an effect on the guest molecules of the complexes, which make them change from L^1 ligands in complex **I** to water molecules in complexes **II** and **III**; (ii) the size and shape of the A and B rings changes greatly. In the structure of **I**, ring A and ring B are obviously rectangular, and in the same plane, the sizes are 7.1646(35) × 3.2877(26) and 3.2877(26) × 2.9862(32) Å, respectively. When the methoxy group changes to ethoxy group, ring A and ring B in structure **II** are twisted and transformed into parallelogram, and their sizes become 7.2991(23) × 3.2196(22) and 3.2196(22) × 2.9074(20) Å. Moreover, dihedral angle between ring A and ring B is 8.851(35)° (Fig. 6d). When ethoxy is changed to butoxy group, due to the increase of steric hindrance, ring A breaks and ring B becomes a regular octagon; (iii) with the increase of substituent length, the spatial extension direction of L^n ligand changes significantly, which makes the structural dimension change from two-dimensional to three-dimensional. In the structures of **I** and **II**, L^1 and L^2 ligands extend infinitely from the direction nearly perpendicular to the A and B rings to form a two-dimensional structure. The dihedral angle formed by L^1 with A and B rings was 83.472(42)° (Fig. 4b), while the dihedral angle of L^2 with A and B rings changed to 89.924(53)° when the substituent changed from methoxy to ethoxy (Fig. 6e). In structure **III**, the L^3 ligands form a dihedral angle (49.588°), which are almost perpendicular to the B rings to form a three-dimensional structure. Meanwhile, the dihedral angles formed by the L^3 ligands and the B rings are 79.772(14)° and 79.708(10)°, respectively (Fig. 6g). In addition, the conjugated rings of L^n (n = 1, 2, 3) ligands also have obvious dislocations (Fig. 7).

CONCLUSIONS

In this work, the coordination polymers with different dimensions were obtained by adjusting the length of substituents of ligands under the same synthetic conditions. This method of adjusting the structural diversity by the length of substituents provides a certain idea for the further development of structural chemistry, and is also an effective attempt in the field of crystal engineering.

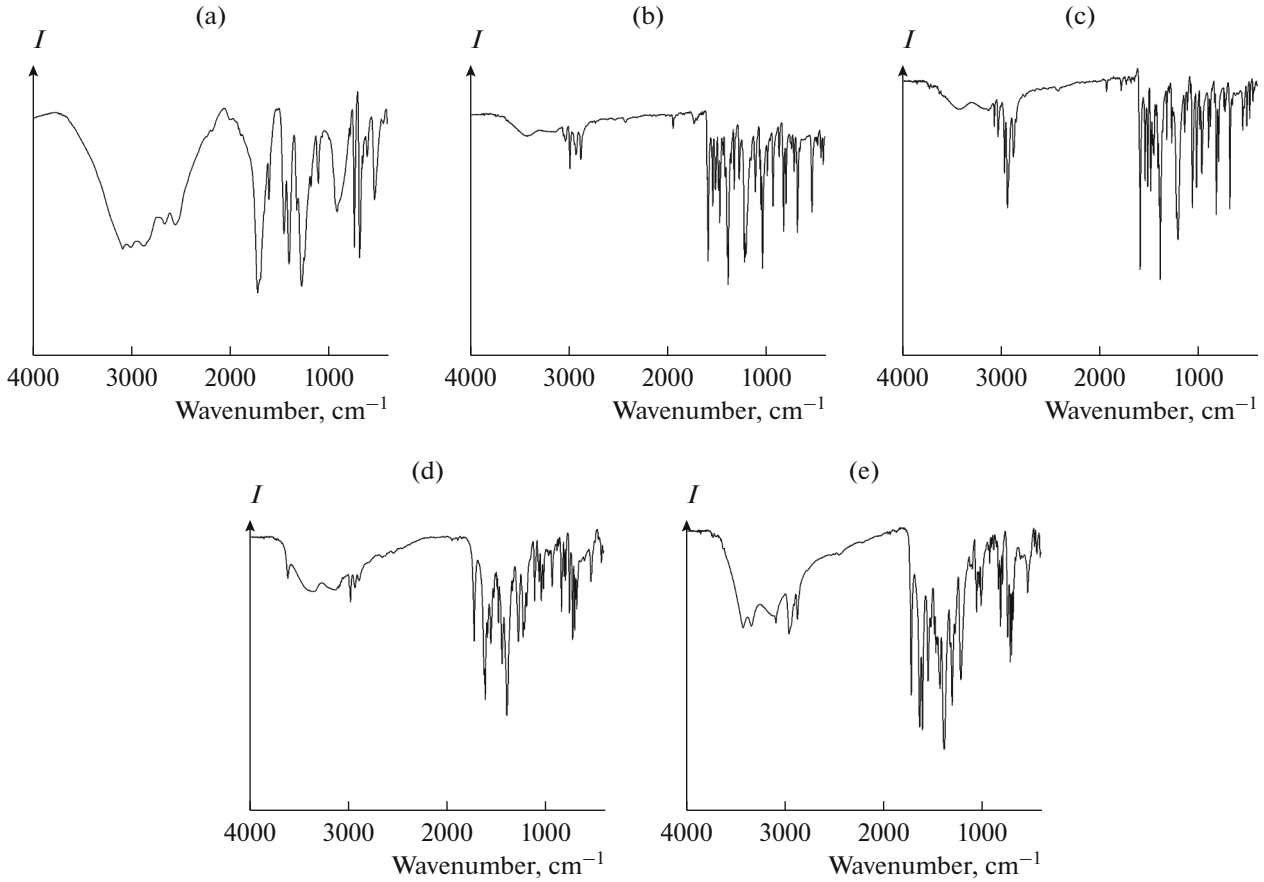

Fig. 4. The IR spectra of ligand BTC (a), ligands L^2 (b), L^3 (c), and complexes **II** (d), **III** (e).

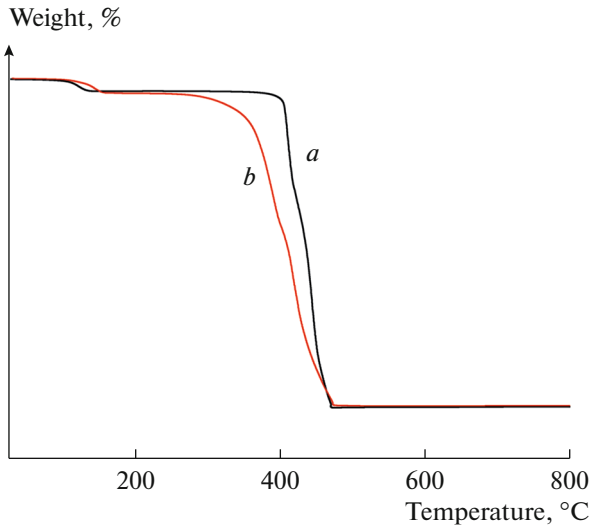

Fig. 5. TGA of complexes **II** (*a*) and **III** (*b*).

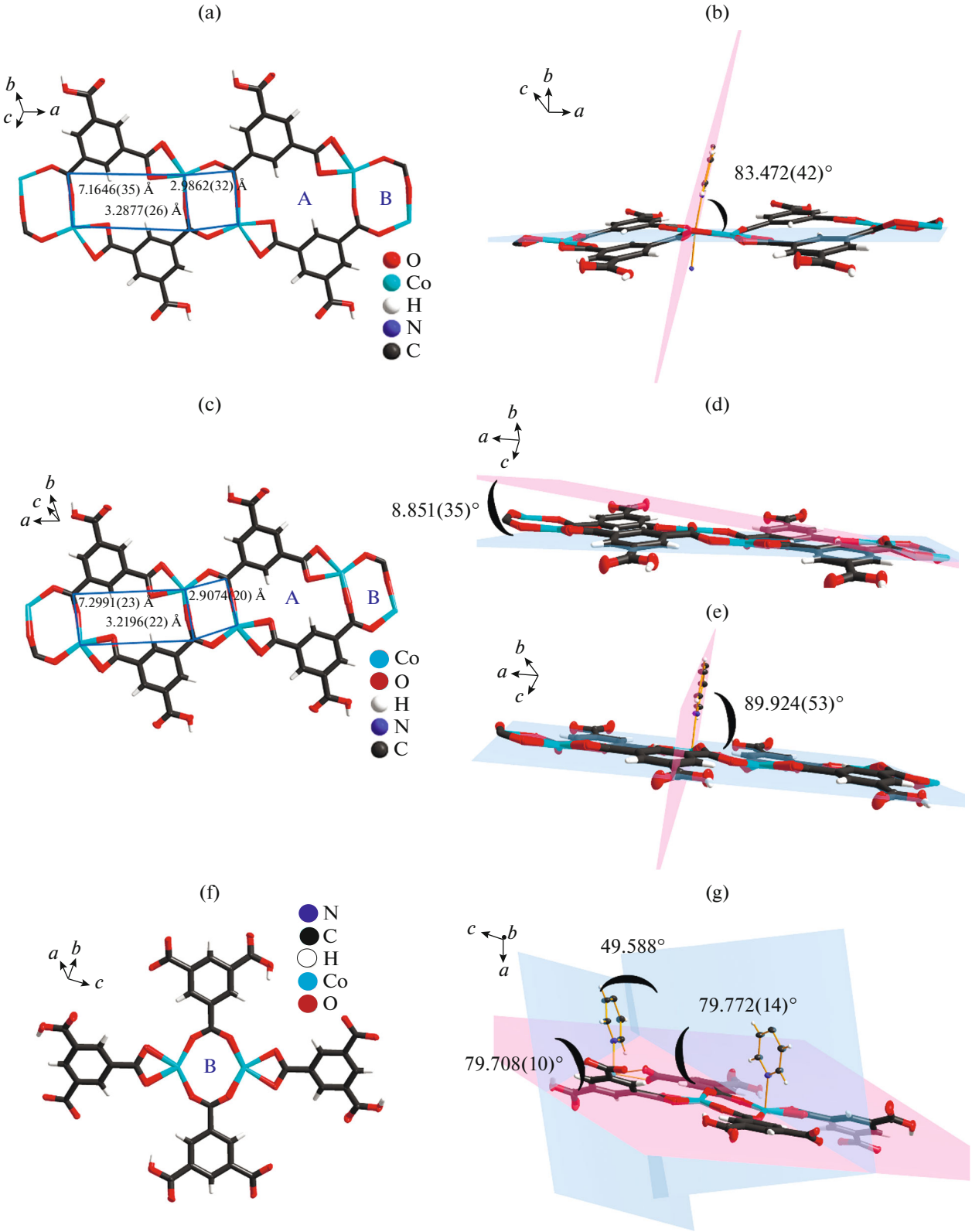

Fig. 6. The rings A and B formed by BTC ligands and cobalt ions in **I** (a); the dihedral angle formed by L^1 with A and B rings in **I** (b); the rings A and B formed by BTC ligands and cobalt ions in **II** (c); the dihedral angle between ring A and ring B in **II** (d); the dihedral angle of L^2 with A and B rings in **II** (e); the ring B formed by BTC ligands and cobalt ions in **III** (f); the dihedral angle between L^3 ligands, the dihedral angles between L^3 ligands and rings B are 79.772(14)° and 79.708(10)°, respectively (g).

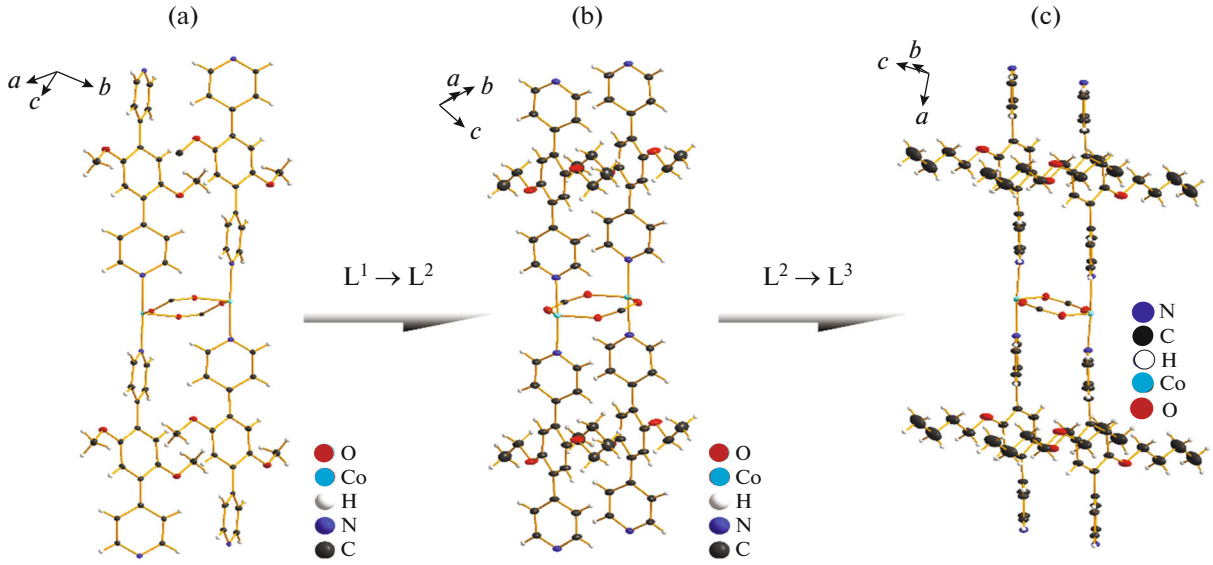

Fig. 7. The conjugated rings of L^1 ligand form dihedral angles to each other in **I** (a); the benzene ring in L^2 ligand forms a dihedral angle with the two pyridine rings in **II** (b); the benzene ring in L^3 ligand forms a dihedral angle with the two pyridine rings in **III** (c).

FUNDING

This work was supported by quality engineering of Anqing Normal University in 2018 (2018aqnujyxm052), anhui provincial quality engineering project in 2019 (2019jyxm0291) and anhui natural science foundation youth project (1908085QB49).

CONFLICT OF INTEREST

The authors declare than they have no conflicts of interest.

REFERENCES

1. Li, Y.Z., Wang, G.D., Shi, W.J., et al., *ACS Appl. Mater. Inter.*, 2020, vol. 12, p. 41785.
2. He, X., Looker, B.G., Dinh, K.T., et al., *ACS Catal.*, 2020, vol. 10, p. 7820.
3. Zhang, P.F., Yang, G.P., Li, G.P., et al., *Inorg. Chem.*, 2019, vol. 58, p. 13969.
4. Zhang, Y., Gutierrez, M., Chaudhari, A.K., et al., *ACS Appl. Mater. Inter.*, 2020, vol. 12, p. 37477.
5. Chen, L.Y., Wang, J.F., Shen, X.S., et al., *Inorg. Chem. Front.*, 2019, vol. 6, p. 3140.
6. Min, H., Han, Z.S., Wang, M.M., et al., *Inorg. Chem. Front.*, 2020, vol. 7, p. 3379.
7. Zhong, W.B., Li, R.X., Lv, J., et al., *Inorg. Chem. Front.*, 2020, vol. 7, p. 1161.
8. Qin, L., Jia, H.J., Guo, Z.J., et al., *Cryst. Growth Des.*, 2014, vol. 14, p. 6607.
9. Chen, S.S., Sheng, L.Q., Zhao, Y., et al., *Cryst. Growth Des.*, 2016, vol. 16, p. 229.
10. Isaeva, V.I., Tarasov, A.L., Chernyshev, V.V., et al., *Mendeleev. Commun.*, 2015, vol. 25, p. 466.
11. Yang, G., Liu, J., Zhou, M., et al., *ACS Sustain. Chem. Eng.*, 2020, vol. 8, p. 1194711955.
12. Mukhopadhyay, A., Jindal, S., Savitha, G., et al., *Inorg. Chem.*, 2020, vol. 59, p. 62026213.
13. Nandi, G., Titi, H.M., Thakuria, R., et al., *Cryst. Growth Des.*, 2014, vol. 14, p. 27142719.
14. Huang, Y.Q., Wan, Y., Chen, H.Y., et al., *New J. Chem.*, 2016, vol. 40, p. 75877595.
15. Chen, D.M., Zhang, N.N., Tian, J., et al., *Inorg. Chem.*, 2017, vol. 56, p. 73287331.
16. Huang, W., Zhang, M., Huang, S.D., et al., *Inorg. Chem.*, 2017, vol. 56, p. 67686771.
17. Li, L.B., Lin, R.B., Krishna, R., et al., *J. Am. Chem. Soc.*, 2017, vol. 139, p. 77337736.
18. Wang, Y.T., Tang, G.M., and Wang, C.C., *Appl. Organomet. Chem.*, 2020, vol. 34, p. e5654.
19. Luo, Q.D., Zhu, Z., Fan, C.B., et al., *J. Mol. Struct.*, 2019, vol. 1188, p. 5761.
20. Liu, G.Y., Huang, X.D., Lu, M., et al., *J. Sep. Sci.*, 2018, vol. 42, p. 14511458.
21. Salehi, S., Anbia, M., and Razavi, F., *Environ. Prog. Sustain.*, 2019, vol. 39, p. 13302.
22. Zou, G.L., Wang, X.L., Li, T.T., et al., *Asian J. Chem.*, 2014, vol. 26, p. 3127.
23. Davies, R.P., Less, R.J., Lickiss, P.D., et al., *Dalton Trans.*, 2007, vol. 24, p. 2528.
24. Yaghi, O.M., Davis, C.E., Li, G., et al., *J. Am. Chem. Soc.*, 1997, vol. 119, p. 2861.
25. Wang, Z., Kravtsov, V.C., and Zaworotko, M.J., *Angew. Chem.*, 2005, vol. 117, p. 2937.

26. Manna, S.C., Mistri, S., and Jana, A.D., *CrystEngComm*, 2012, vol. 14, p. 7415.
27. Cai, Y., Zhang, Y., Huang, Y., et al., *Cryst. Growth Des.*, 2012, vol. 12, p. 3709.
28. Zhang, C.L., Li, Y.L., Xu, et al., *Chem. Eur. J.*, 2018, vol. 24, p. 27.
29. Takaoka, K., Kawano, M., and Tominaga, M., *Angew. Chem. Int. Ed.*, 2005, vol. 44, p. 2151.
30. *APEX2, SAINT, and SADABS*, Madison: Bruker AXS Inc., 2005.
31. Blatov, V.A. and Shevchenko, A.P., *TOPOS. Version 4.0*, Samara: Samara State Univ., 2006.
32. *APEX2, SAINT and SADABS*, Madison: Bruker AXS Inc., 2012.
33. *Oxford Diffraction, CrysAlis PRO,* Yarnton, Oxfordshire: Oxford Diffraction, Ltd., 2010.
34. Sheldrick, G.M., *Acta Crystallogr., Sect. A: Found. Adv.*, 2015, vol. 71, p. 3.
35. Sheldrick, G.M., *Acta Crystallogr., Sect. A: Found. Crystallogr.*, 2008, vol. 64, p. 112.
36. Sheldrick, G.M., *Acta Crysallogr. Sect. C: Struct. Chem.*, 2015, vol. 71, p. 3.